

# Sensitivity of astrometry and photometry estimation to spatial variations of the PSF

O. Beltramo-Martin<sup>a,b</sup>, G. Witzel<sup>c</sup>, A. Ciurlo<sup>d</sup>, P. Turri<sup>e</sup>, and J. Lu<sup>e</sup>

<sup>a</sup>ONERA, The French Aerospace Laboratory, Marseille, France

<sup>b</sup>Aix Marseille Univ., CNRS, CNES LAM, Marseille, France

<sup>c</sup>Max-Planck-Institute for Radioastronomy, Bonn, Germany.

<sup>d</sup>Department of Physics and Astronomy, UCLA, Los Angeles, CA 90095-1547, United States

<sup>e</sup>Department of Astronomy, UCB, Berkeley, CA 94720-3411, United States

## ABSTRACT

Adaptive optics (AO) restore the angular resolution of ground-based telescopes, but at the cost of delivering a time- and space-varying point spread function (PSF) with a complex shape. However, the characterization of the PSF spatial variations is crucial to maintain photometric and astrometric accuracy at the same level across the field. Two effects are playing a major role in those variations: (i) the atmospheric anisoplanatism that takes its origin in the spatial decorrelation of the AO-compensated phase (ii) the field-dependent static aberrations caused by the telescope and the internal optical elements of the system. We aim at analyzing the sensitivity of science metrics with respect to modeling inaccuracies of the PSF variations. Additionally, we want to determine constraints on the modeling and calibration accuracy of the anisoplanatism/static aberrations field variations for the desired level of accuracy of astrometric/photometric parameters. We present an analysis through the AIROPA (Anisoplanatic and Instrumental Reconstruction of PSFs for AO) pipeline based on data from the near-infrared imager NIRC2 at Keck that shows that the anisoplanatism is sufficiently described over 3 layers in K-band, while the static phase variations is dominated by a focus term, indicating the presence of a field curvature aberration within the system. We analyze how atmospheric profile vertical resolution and field curvature effects translate into errors on stellar parameters estimation and propose calibration strategies accordingly.

**Keywords:** AIROPA, Adaptive optics, PSF reconstruction, Galactic center, Keck

## 1. INTRODUCTION

Precise photometry and astrometry in crowded fields encounter the problem of Point Spread Function (PSF) determination due to the sources crowding, which limits the final reachable accuracy on stellar parameters.<sup>1,2</sup> In order to enhance astrometric measurements, Adaptive-optics (AO) is deployed for sharpening the PSF. However, AO introduces PSF spatial and temporal variability, which necessitates to implement specific post-processing tools dedicated to AO-corrected images to reach the maximal accuracy as possible. A straightforward option consists in segmenting the image into areas where the PSF is supposed to be constant, but the PSF can not be identified at any segment location because noise and crowding limitations. Also, extracting the PSF at the image edges where the field is potentially sparser is not completely satisfactory if one does not account for PSF spatial variations.

This is in this context that a large effort is being led at the University of California and W.M. Keck Observatory to provide a PSF reconstruction (PSF-R) pipeline to model the PSF at any position of the field and spectrum using AO control loop data,<sup>3,4</sup> dedicated calibration of field-dependent static aberrations<sup>5</sup> and model of the spatial inhomogeneity of the PSF due to atmospheric effects, so-called the anisoplanatism effect.<sup>6,7</sup> This on-going work has permitted the emergence of a new pipeline known as AIROPA,<sup>8,9</sup> which is a PSF extrapolation and profile-fitting software based on StarFinder.<sup>10</sup> It combines a model of PSF spatial variations with the native detection and extraction facility of Starfinder. Instead of segmenting the image, the full frame is processed by constraining the PSF shape according to its position in the field through the modeling of

---

Further author information: olivier.beltramo-martin@lam.fr

- 1 the anisoplanatism that manifests as a focal-angular term coming from the use of a laser Guide Star (LGS) on-axis, plus a tip-tilt anisoplanatism introduced by the phase spatial decorrelation between the tip-tilt Natural Guide Star (NGS) (which is usually 20-25" off from the field center) and the scientific field. The atmospheric vertical distribution model relies so far on the MASS/DIMM<sup>11</sup> that delivers a 7-layer  $C_n^2(h)$ .
- 2 Field-dependent static instrumental aberrations which are measured ahead of time with phase diversity thanks to a fiber moving in the entrance system focal plane.<sup>5</sup>

AIROPA has shown excellent results in simulation, with improvements by a factor 3 on astrometry up to 8 on photometry,<sup>8</sup> which has not been verified on-sky yet. Therefore, our purpose is to identify what could be the origin of this mis-performance through a sensitivity analysis. For instance, the MASS/DIMM is known to have a limited vertical resolution, is it sufficient for NIRC2 application or does it contribute to limit estimates accuracy? Should we preferably investigate for an alternative method, such as the Focal Plane Profiling (FPP) that identifies the  $C_n^2(h)$  from the image itself<sup>12</sup>? Moreover, the field-dependent static aberrations are measured using a fiber stage, is the control of this stage good enough to not bias the PSF model? We present the PSF model framework in Sect. 2 and the sensitivity analysis in Sect. 3.

## 2. POINT SPREAD FUNCTION DESCRIPTION

### 2.1 Off-axis extrapolation

The off-axis PSF is well approximated in the Fourier domain as the multiplication of the on-axis Optical transfer Function (OTF) with spatial filters as follows

$$\tilde{h}(\boldsymbol{\rho}/\lambda, \theta) = \tilde{h}_0(\boldsymbol{\rho}/\lambda) \times \tilde{k}_{\text{stat}}(\boldsymbol{\rho}/\lambda, \theta) \times \tilde{k}_{\text{an}}(\boldsymbol{\rho}/\lambda, \theta_{\text{lgs}}, \theta_{\text{ngs}}, \theta, C_n^2(h)), \quad (1)$$

where  $\tilde{h}_0$  is the on-axis OTF, that depends on the angular frequencies vector  $\boldsymbol{\rho}/\lambda$  and contains the AO residual, on-axis telescope/co-phasing/instrument static aberrations and the uncompensated atmospheric frequencies. Filters in Eq. 1 permit to extrapolate the PSF at any position in the field by including

- $\tilde{k}_{\text{stat}}$  that accounts for spatial variations of static aberrations in the field. This filter is calibrated on the near infra-red NIRC2 at Keck II by using phase diversity techniques on an internal fiber source.<sup>5</sup> The fiber was positioned at different z position values (+2 mm, +4 mm and +6 mm) and at several (x,y) locations in the instrument entrance focal plane to map the static phase across the field. This process has provided 9×9 maps distributed over a square field of view with 1 arcsec-resolution to sample the field, which covers the NIRC2 field of view in narrow field mode.
- $\tilde{k}_{\text{an}}$  that refers to the anisoplanatism effect and is well described through the multiplication of a two separated filters as follows

$$\tilde{k}_{\text{an}}(\boldsymbol{\rho}/\lambda, \theta_{\text{lgs}}, \theta_{\text{ngs}}, \theta, C_n^2(h)) = \tilde{k}_{\text{lgs}}(\boldsymbol{\rho}/\lambda, \theta_{\text{lgs}} - \theta, C_n^2(h)) \times \tilde{k}_{\text{ngs}}(\boldsymbol{\rho}/\lambda, \theta_{\text{ngs}} - \theta, C_n^2(h)) \quad (2)$$

where  $\tilde{k}_{\text{lgs}}$  is the focal-angular anisoplanatism filter, which depends of the LGS position  $\theta_{\text{lgs}}$  and  $\tilde{k}_{\text{ngs}}$  the anisoplanatism filter as a function of the NGS position  $\theta_{\text{ngs}}$ . Both these filters are  $C_n^2(h)$ -dependent and a way to compute them is given in.<sup>6</sup>

Modeling the PSF at any field location can be achieved by coupling a PSF extraction software to identify  $\tilde{h}_0$  and a precise calibrated spatial variations model as it is aimed by AIROPA. Alternatively, one may also estimate the on-axis PSF by using PSF reconstruction,<sup>3,4,13-17</sup> or PSF parametric models,<sup>18,19</sup> which is kept for future work.

We present in Fig. 1 the photometry error obtained on simulated images of the Galactic center observed with NIRC2 with AIROPA. Two modes have been tested (i) the single mode for which the PSF is considered as constant across the field (ii) the variable mode that relies on the PSF spatial variations model described in Eq. 1. From the simulation, we know exactly what are the number of stars and their stellar parameters, as well as the description of the anisoplanatism and field-dependent static aberrations. We clearly show that not taking into account the PSF spatial variations introduces a strong field-dependent bias and degrades the accuracy by at least a factor 3, advocating for the need of characterizing field-dependent aberrations.

# SINGLE PSF

# VARIABLE PSF

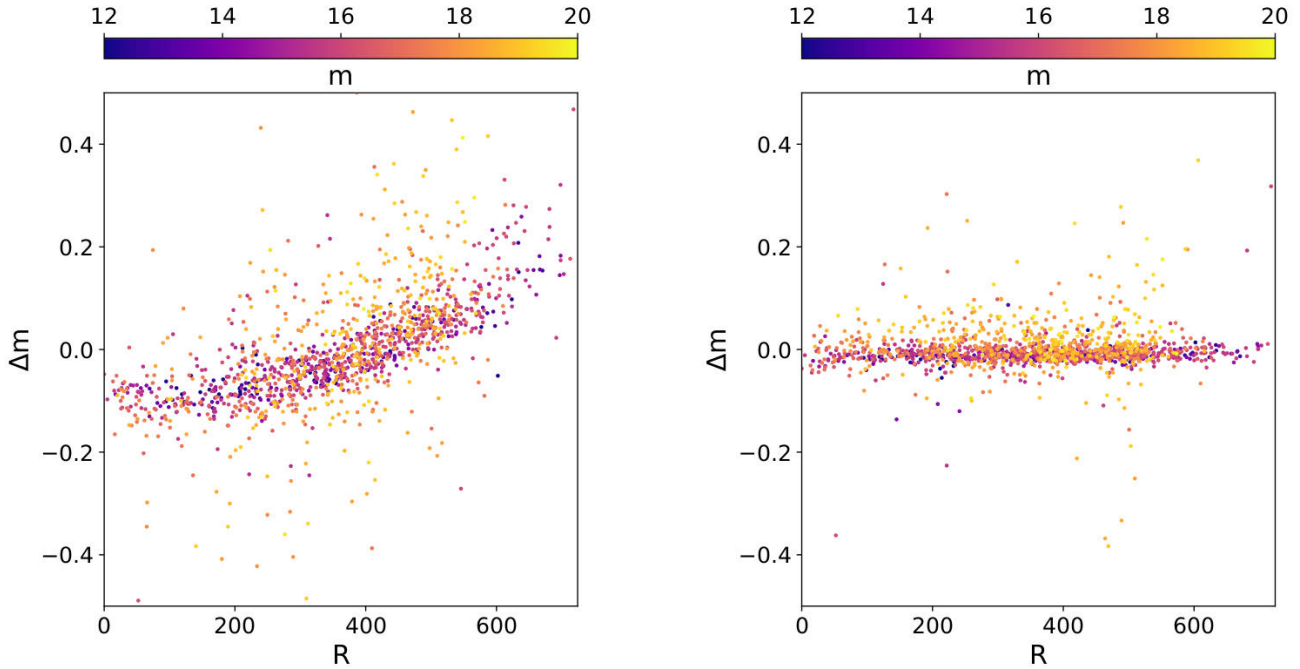


Figure 1: Photometry error obtained on simulated images of the Galactic center observed with NIRC2, as function of the off-axis distance in pixels obtained with the single (constant PSF) and variable (spatial variations included) mode of AIROPA.

## 2.2 Analysis of field-static aberrations

According to on-sky observations, the anisoplanatism does not play a major role in the PSF spatial variations observed with NIRC2. This is somehow expected regarding that i) the NIRC2 field diameter is limited to  $10 \text{ arcsec} \times 10 \text{ arcsec}$  ii) the isoplanatic angle  $\theta_0$ <sup>20</sup> reaches 20 up to 30 arcsec in K-band, which suggests that NIRC2 observes an isoplanatic field most of the time. Only under specific conditions of bad seeing and a large telescope zenith angle (usually 40-45 degrees to observe the GC at Mauna Kea), the anisoplanatism can produce a significant change of the PSF morphology, which remains rare, though. Consequently, a particular care of field-dependent static must be given.

We present in Fig. 2 the phase diversity results that shows the 81 maps measured every 1 arcsec by using the FeII filter ( $1.6455 \mu\text{m}$ ). In absence of telescope, the on-axis static aberration has a rms value of 90 nm, which seems to comply with S. Ragland calibration.<sup>3</sup> Off-axis aberrations reach 200 nm rms at the field corner, which degrades the Strehl-ratio (SR) down to 72% in K-band ( $2.2 \mu\text{m}$ ). We observe the presence of a longitudinal pattern on each map that contains quite high spatial frequencies. It maybe introduced by scratches on the Deformable Mirror (DM) for instance, but the origin can not be easily determined without specific measurements. We also notice a strong degradation when getting off-axis as it is highlighted by the static OPD rms value.

Fig. 2 illustrates that the focus term looks to increase with respect to the azimuthal position. To provide evidence of this observation, we have reconstructed 500 Zernike modes for each of the 81 maps. We present in Fig. 3 reconstruction results on and off-axis, that shows an excellent reconstruction with residual error of 30 nm rms regardless the azimuthal position. The fact that the residual error does not evolve with respect to the field location indicates that the spatial variations of static aberrations are composed by low order modes mostly. We have a confirmation when looking at Fig. 4: it shows that the reconstructed focus term drops from -20 nm down to -180 nm at 6, arcsec-off from the on-axis, which advocates for the presence of a field curvature effect within the

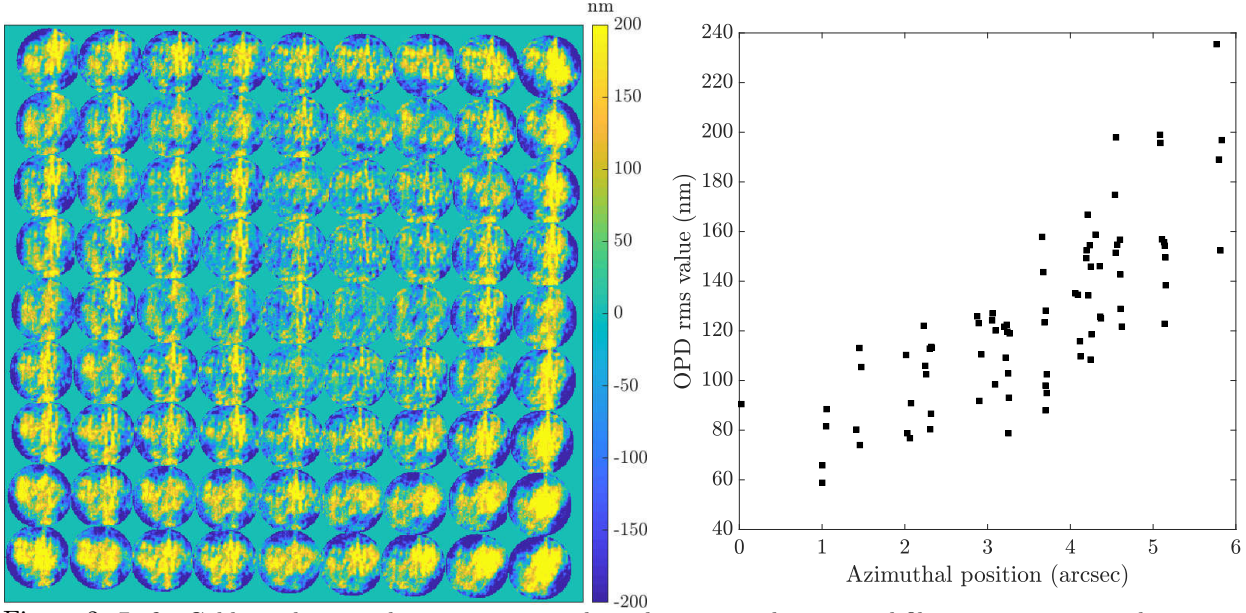


Figure 2: **Left:** Calibrated static phase maps using phase diversity with a internal fiber source positioned every 1 arcsec within the NIRC2 field of view. **Right:** Static OPD rms value with respect to the azimuthal position within the field.

system. From a quadratic polynomial regression, we obtain the following model for the focus term degradation

$$a_4(\alpha) = 3.6 \text{ nm/arcsec}^2 \times \alpha^2 - 17 \text{ nm}, \quad (3)$$

where  $\alpha$  is the azimuthal position in the field in arcsec. So far, it is not clear whether this field curvature effect is real or a part of it is due to variations of the z-position of the fiber during the static phase maps calibration. If this effect is a pure calibration artifact, we should improve photometry/astrometry results by removing it from the static maps as it will be tested in future work.

### 3. SENSITIVITY ANALYSIS WITH AIROPA

#### 3.1 Simulations framework

The point of this section is know to understand how sensitive are science metrics, i.e. photometry and astrometry, to mis-modeling of PSF spatial variations. To do so, we have followed the present strategy

- **Step 1:** We simulate a grid of PSFs positioned every 1 arcsec in the field (fiber positions), that we denote as the *reference PSF grid*. The on-axis OTF is obtained from a deep on-sky observation using the K cont filter in laser-assisted mode and we used Eq. 1 to extrapolate the OTF spatially, knowing the  $C_n^2(h)$  and including static maps. The anisoplanatism model is practically calculated from the methodology explained in<sup>6</sup> and relies on a 250 m-resolution profile obtained at Paranal.<sup>21</sup> It is true that we should run this process with the specific profile at Mauna Kea, but there is not such a highly resolved profile there in my knowledge. Note that PSF grids are not obtained from end-to-end simulations, but from a mix between an on-axis image obtained on-sky plus long-exposure model of the anisoplanatism plus the static aberrations calibration. We present the PSF grid and the final image in Fig. 5.
- **Step 2:** We interpolate the PSF grid at a finer angular sampling within the field of view to comply with AIROPA specifications and simulate the corresponding GC image (2000 stars), including detector noises and shot noise from the star and the sky.
- **Step 3:** We create another PSF grid, a *priori PSF grid*, by modifying the inputs, like the atmosphere vertical distribution or the field curvature effect, in order to introduce a model error into our prior on the PSF morphology.

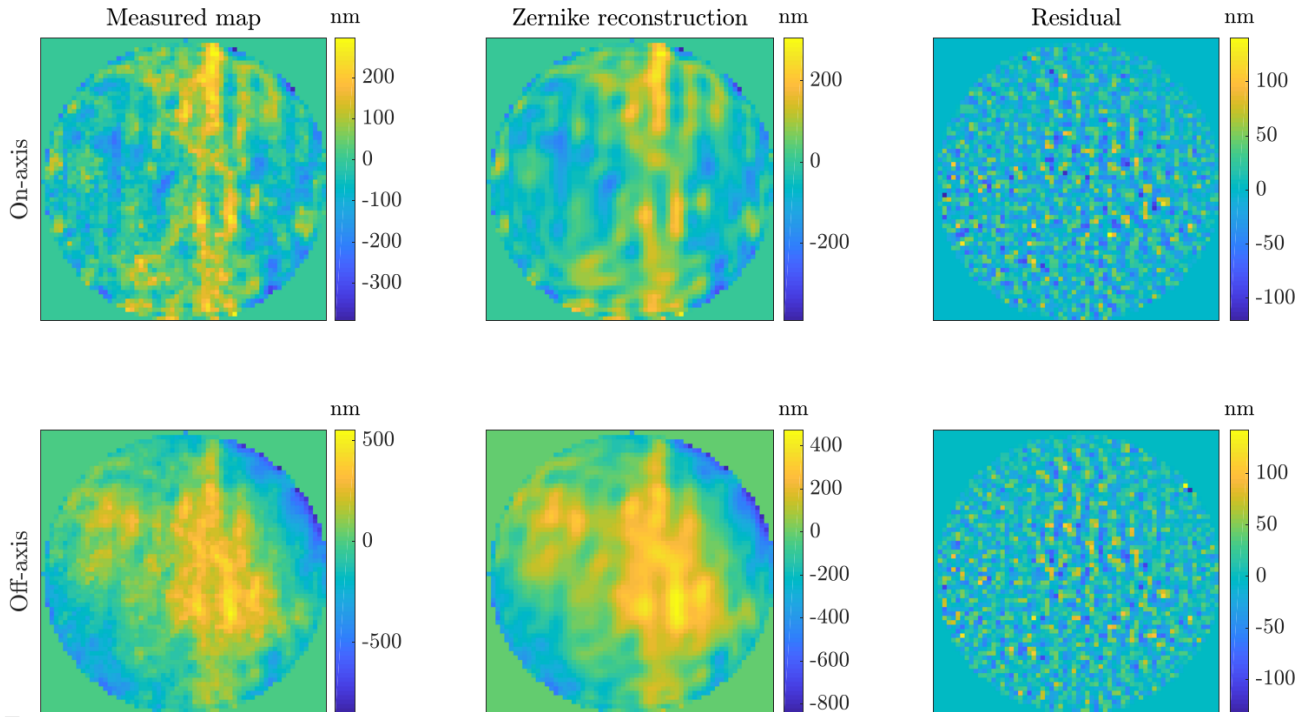


Figure 3: **Left:** Measured static maps on-axis (top) and at the field corner (bottom) **Middle:** Average of Zernike reconstructed maps over 500 modes. **Right:** Residual

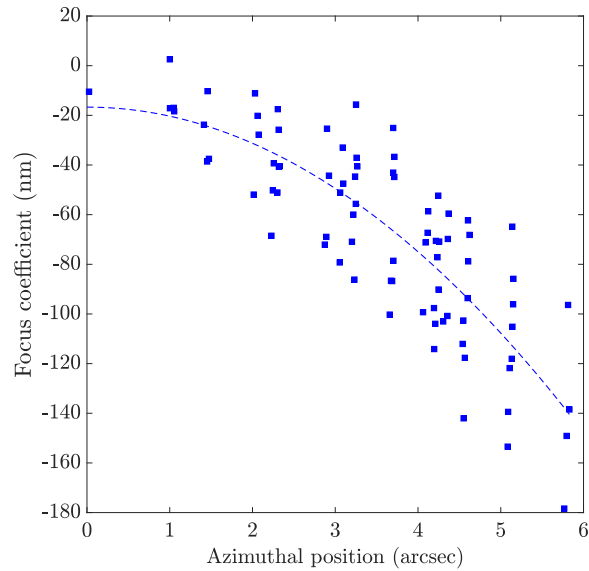


Figure 4: Reconstructed focus term rms value with respect to the fiber azimuthal position within the field. The dotted line corresponds to a quadratic regression.

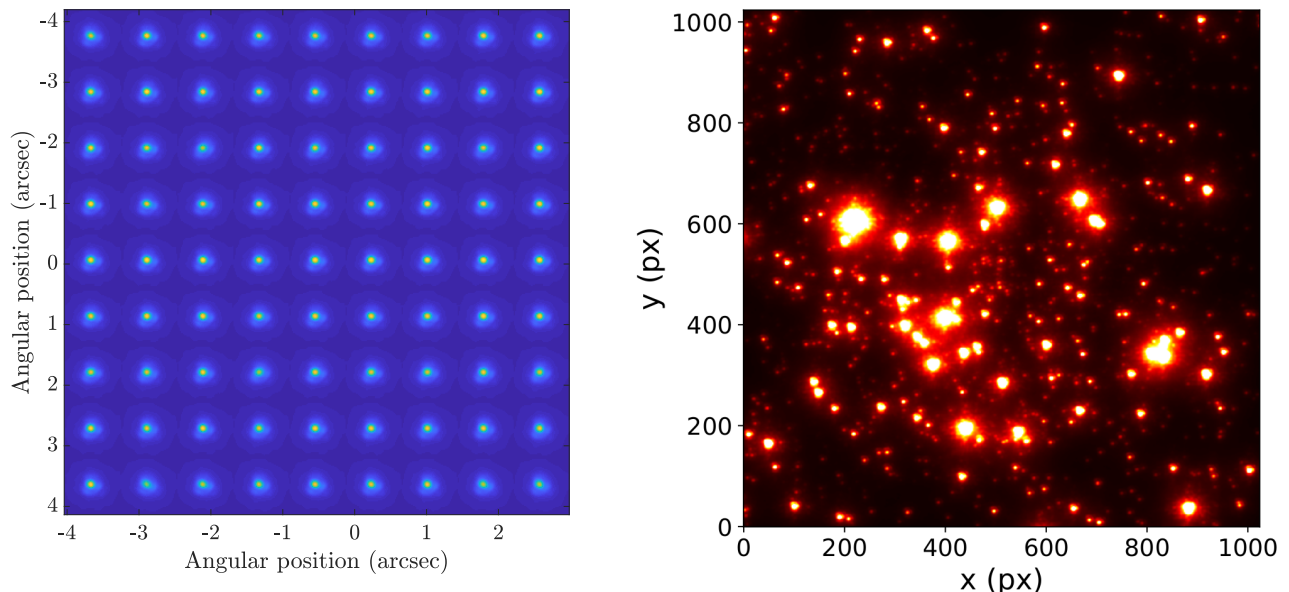


Figure 5: **Left:** Concatenation of simulated PSFs **Right** Corresponding simulated GC image using the median atmospheric conditions at Mauna Kea and the calibrated field-dependent static maps.

- **Step 4:** We pass this new PSF grid to AIROPA to measure stellar parameters that are compared to catalog values utilized to generate the GC image. The case where the *a priori PSF grid* and the *reference PSF grid* are the same gives the best accuracy values. We make deviate the *a priori PSF grid* from the reference more and more and see how this translates into degradation of stellar parameters accuracy.
- **Step 5:** We decide what is the maximal deviation of the model from the truth we can tolerate with respect to a criterion on the science metrics accuracy.

### 3.2 Sensitivity to field curvature modeling

The simulated PSF grid involved in step 1 includes only the field curvature model described in Eq. 3, the other Zernike modes than focus are omitted. We introduce the factor  $k = 3.64 \text{ nm/arcsec}^2$  as the field curvature coefficient that connects the rms value of the defocus wavefront with the azimuthal position in the field. This factor has been estimated from a polynomial regression as explained in Sect. 2.2. During step 3, we have played on the value of  $k$ , from 0 to  $5.5 \text{ nm/arcsec}^2$ , in order to modify the strength of the field curvature effect. We present the corresponding photometry and astrometry errors in Fig. 6. Errors are averaged out for different ranges of stars magnitude. Results put into light that we reach in average  $0.007 \text{ mag}$  and  $100 \mu\text{as}$  of accuracy, which is barely comparable to what is obtained in best conditions on-sky. As expected, we see the lessening of the accuracy when deviating the field curvature model from the truth, for two cases (i)  $k_{\text{ref}} = 3.64 \text{ nm/arcsec}^2$  as measured on static maps (ii)  $k_{\text{ref}} = 0$ , i.e. there is no field curvature in the simulated GC image. We would like to stress that this analysis supposes median atmospheric conditions. If the seeing value is worse than that, the anisoplanatism will have more impact which will lessen the influence of the field curvature model in the final science metrics accuracy. Moreover, the on-axis PSF was given for a specific observation and AO status. Some reasons may intervene to diminish the AO performance, such as residual jitter introduced by wind shake, which would also decrease the importance of well estimating the field curvature effect. Values will give here must be considered as reasonable order of magnitude for median observation conditions.

So as to determine what must be the accuracy on the fiber stage z-position, we use the following equation

$$z = 8 \times a_4 \times 2\sqrt{3} \times f_{\#}^2, \quad (4)$$

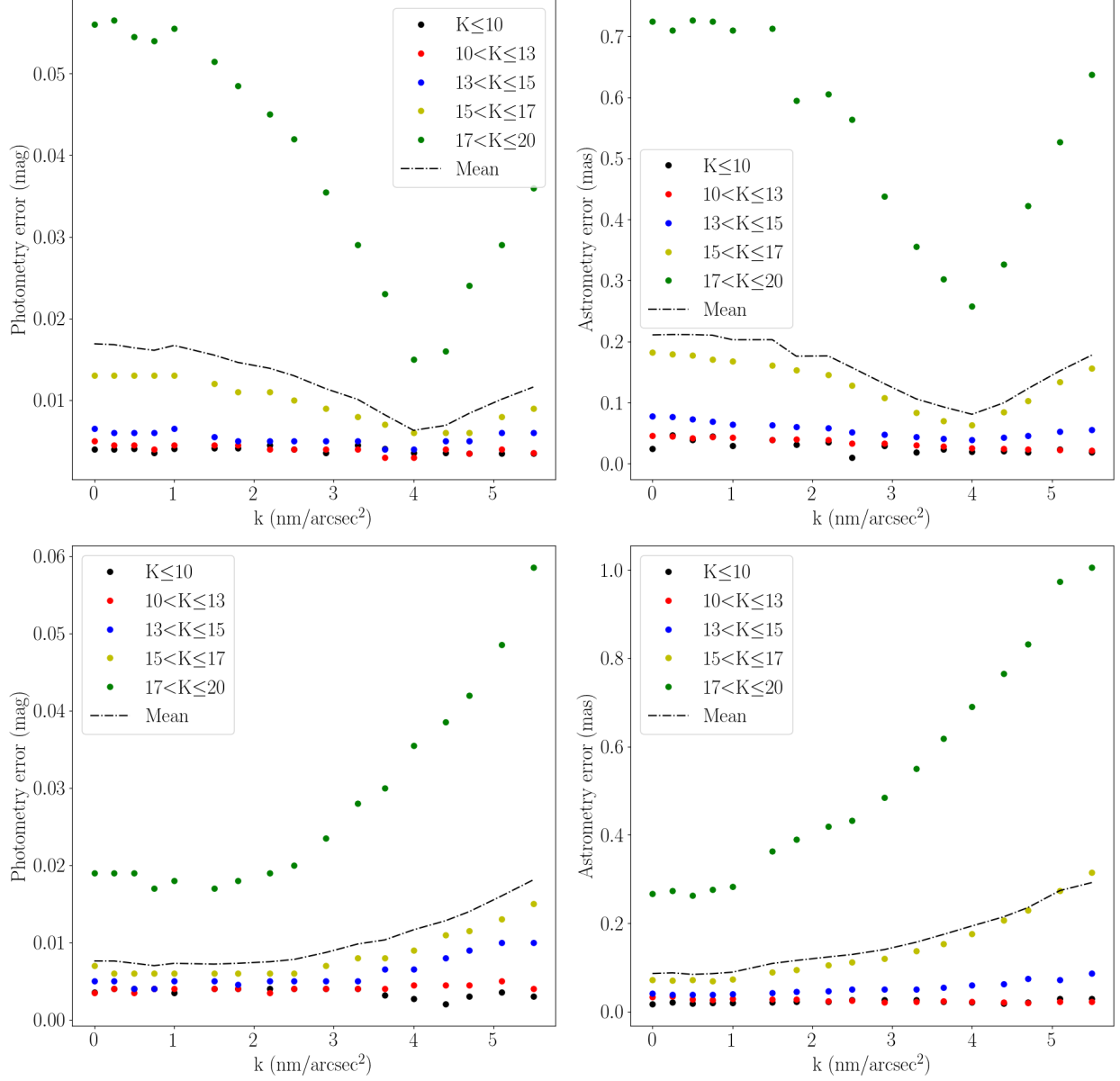


Figure 6: Photometry and astrometry accuracy with respect to the field curvature coefficient taken as prior during step 3. **Top:** the true value is  $k_{\text{ref}} = 3.64 \text{ nm/arcsec}^2$  **Bottom:** the true value is  $k_{\text{ref}} = 0$ .

where  $f_{\#} = 13.43$  is the telescope f ratio and  $a_4$  is the rms value of the defocus term introduced with the fiber stage. From Fig. 6, we can identify  $k_{\text{lim}}$  as the value of field curvature coefficient that generates intolerable error on science metrics. For instance, for  $k_{\text{ref}} = 0$ , mean photometry accuracy is reached for  $k_{\text{lim}} = 3.5 \text{ nm/arcsec}^2$ . Using Eq. 3 and Eq. 4 we have

$$\Delta z(\alpha) = 8 \times |k_{\text{lim}} - k_{\text{ref}}| \times \alpha^2 \times 2\sqrt{3} \times f_{\#}^2, \quad (5)$$

which gives the required accuracy on the fiber stage z-position as function of  $k_{\text{ref}}$  and the position in the field  $\alpha$ . We report in Fig. 7 the z-position accuracy we must achieve as function of the relative error on science metrics at the field border, i.e.  $\alpha = 512 \times \sqrt{(2)} \times 0.00994 = 7.07 \text{ arcsec}$ . Values are obtained by choosing different metrics, such as the mean photometry and astrometry over all stars or only on the faintest ones with  $m_K > 17$ .

Moreover, the fiber stage is presumed to be controllable at a  $10 \mu\text{m}$ -level. From this, one may derive the corresponding error on metrics we can introduce when calibrating the static aberrations. From Eq. 3 the relation with respect to  $\alpha$  is known and we can translate this  $10 \mu\text{m}$  accuracy into errors on stellar parameters as function of the field position, as illustrated in Fig. 7. We see that as long as the fiber stage position is known at a  $10 \mu\text{m}$ -level certainty, stellar parameters may be retrieved at 1% in averaged across the whole field. For fainter stars, this is only ensured in a field of view of 3 arcsec and the error can probably increase up to 6% at the field edges.

Finally, when looking at the case  $k_{\text{ref}} = 0$  and  $k_{\text{lim}} = 3.64 \text{ nm/arcsec}^2$ , we obtain error of 0.0033 mag and  $90.3 \mu\text{s}$  of respectively photometry and astrometry error over all stars, which grows up to 0.013 mag and  $354 \mu\text{s}$  when looking at stars with  $m_K > 17$  only. As a conclusion, if the field curvature we see on Fig. 4 is not real, it should degrade significantly the on-sky results. Similarly, subtracting the field curvature model out from the calibrated maps should have a negative impact on science metrics as well if this effect is real. This will be one of next tests.

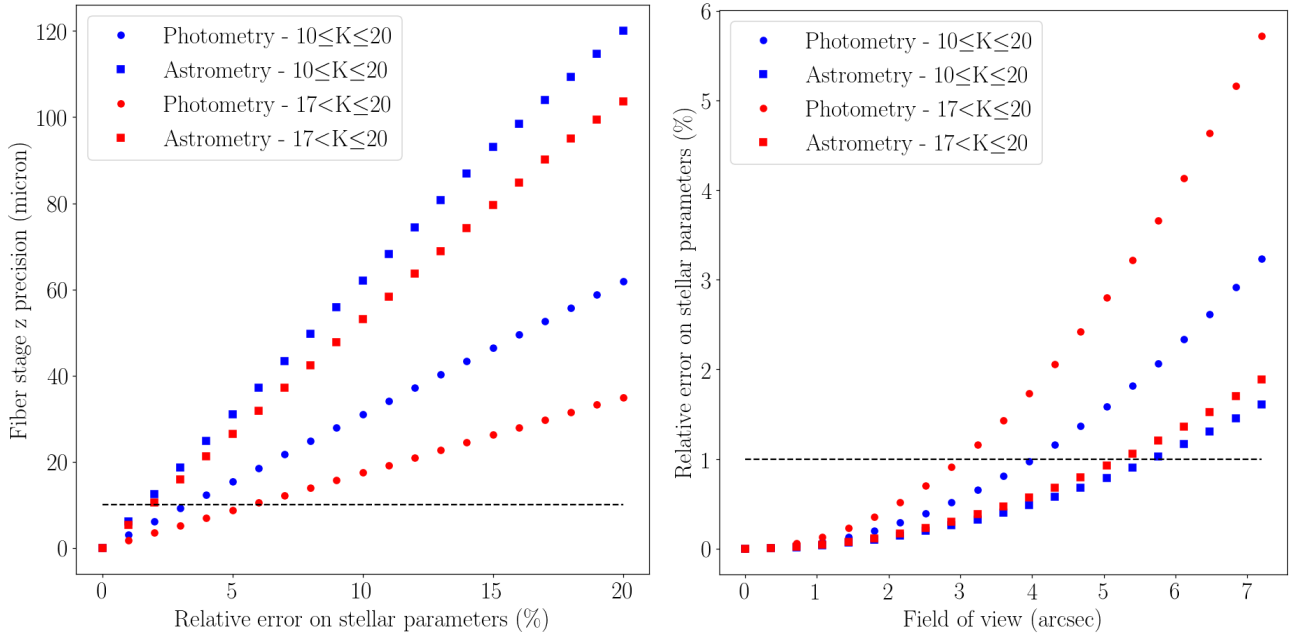


Figure 7: Retrieved accuracy on **Left**: the z-position of the fiber stage with respect to the relative error on  $k$  in the field curvature model **Right**: the science metrics as a function of the position in the field.

### 3.3 Sensitivity to anisoplanatism characterization

We present in Fig. 8 three 35-layers profiles we have considered for this analysis and obtained by statistical measurements at Paranal. The  $C_n^2(h)$  value is calculated as the fractional weight of the layer multiplied by  $r_0^{-5/3}$

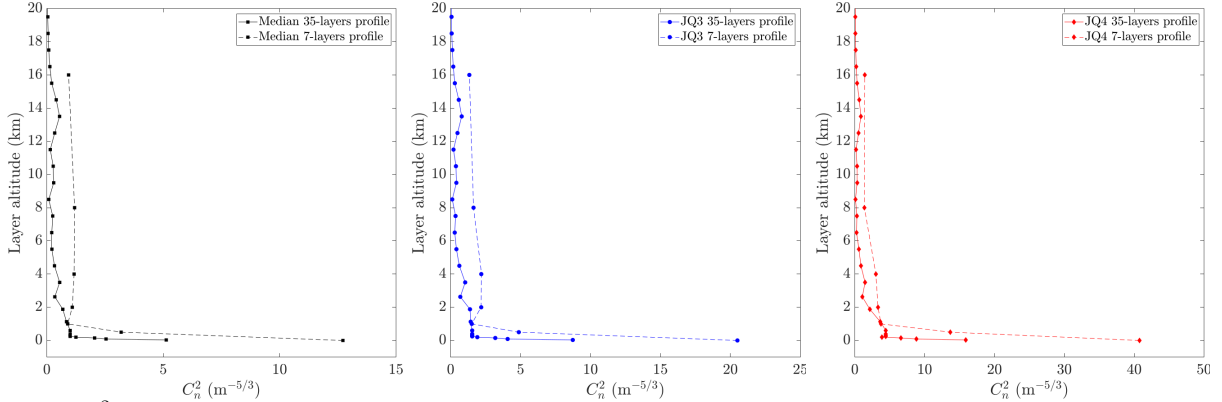


Figure 8:  $C_n^2$  profiles described over 35 layers and then compressed to the MASS/DIMM resolution for (left:) median condition -  $r_0(500\text{ nm}) = 16\text{ cm}$  and  $\theta_0(2.2\mu\text{m}) = 40\text{ arcsec}$  (middle) third quantile -  $r_0(500\text{ nm}) = 12\text{ cm}$  and  $\theta_0(2.2\mu\text{m}) = 28\text{ arcsec}$  (right) fourth quantile -  $r_0(500\text{ nm}) = 8\text{ cm}$  and  $\theta_0(2.2\mu\text{m}) = 26\text{ arcsec}$ .

at 500 nm and for a zenith pointing. We distinguish the median profile as third and fourth quantiles (most pessimist cases) as well.

We present then in Fig. 9 the stellar parameters accuracy as function of the telescope zenith angle and the stars magnitude range. Results are given for the three 35-layers vertical profiles. The reference and prior PSF grids were identical; therefore what we show is the best photometry/astrometry accuracy. Firstly, averaged minimal errors on photometry and astrometry are very similar regardless the profile and reach down to 0.01 mag and 120  $\mu\text{as}$  despite the PSF spatial variations are well known. If we focus on bright stars ( $m_K < 15$ ) only, we obtain better results with 0.005 mag and 60  $\mu\text{as}$ . A further step must be done to understand the origin of this residual error: does it come from best-fitting issues with AIROPA, is it the photon noise limitation or a mixture of both ? Noise-free simulations will put us on the good track to have insights on this.

Moreover, averaged errors degrade with respect to the telescope zenith angle by a factor 5 and 10 on respectively photometry and astrometry from 0 to 60 degrees and once again, despite the perfect knowledge of PSF spatial variations. For instance, at 45 degrees of zenith angle, we reach 0.016 mag and 215  $\mu\text{as}$  of accuracy, which corresponds to an increasing of 60 % and 80 % of respectively photometry and astrometry measurements accuracy ro  $r_0 = 8\text{ cm}$ . These numbers reduce to 30 % for median atmospheric conditions with 0.013 mag and 156  $\mu\text{as}$ . One must conclude that bad PSF model determination is probably not the main limitation of AIROPA to provide accurate measurements.

Now, we consider the problem of the MASS/DIMM vertical resolution. A first analysis has consisted in compressing the  $C_n^2(h)$  vertical distribution over 7-layers only. To do so, we have split the profile in 7 areas centered around heights the MASS/DIMM is sensitive to (0, 0.5, 1 2 4 8 and 16 ,km), then averaged values. The seeing is conserved through this process but not the isoplanatic angle: with median conditions, we get  $\theta_0 = 34\text{ arcsec}$  while it stands to 25 arcsec using the uncompressed profile. We have passed the 7-layers profile-based PSF grid to AIROPA in order to introduce inaccurate characterization of the anisoplanatism. We report results in Fig. 10 that shows an increasing of estimation errors as expected. As a summary, for best conditions ( $r_0 = 16\text{ cm}$ , zenith pointing and bright stars), the limited vertical resolution increases photometry and astrometry errors by respectively 15 % and 30 %. At 45 degrees of zenith angle, errors degrades by a factor 2 at least for median atmospheric conditions, up to a factor 3 for worst seeing conditions.

However, when compressing the  $C_n^2(h)$  using the mein-weighted technique<sup>22</sup> that conserves the isoplanatic angle and the seeing as well, we realize, as presented in Fig. 11, that errors stick to near their minimal values down to 3 layers reconstructed. In other words, the vertical resolution is not specifically a problem for characterizing PSF spatial variations within a 10 arcsec  $\times$  10 arcsec field of view. We only need three layers to introduce enough spatial diversity to reproduce the PSF morphology, at a sufficient level to maintain estimates accuracy

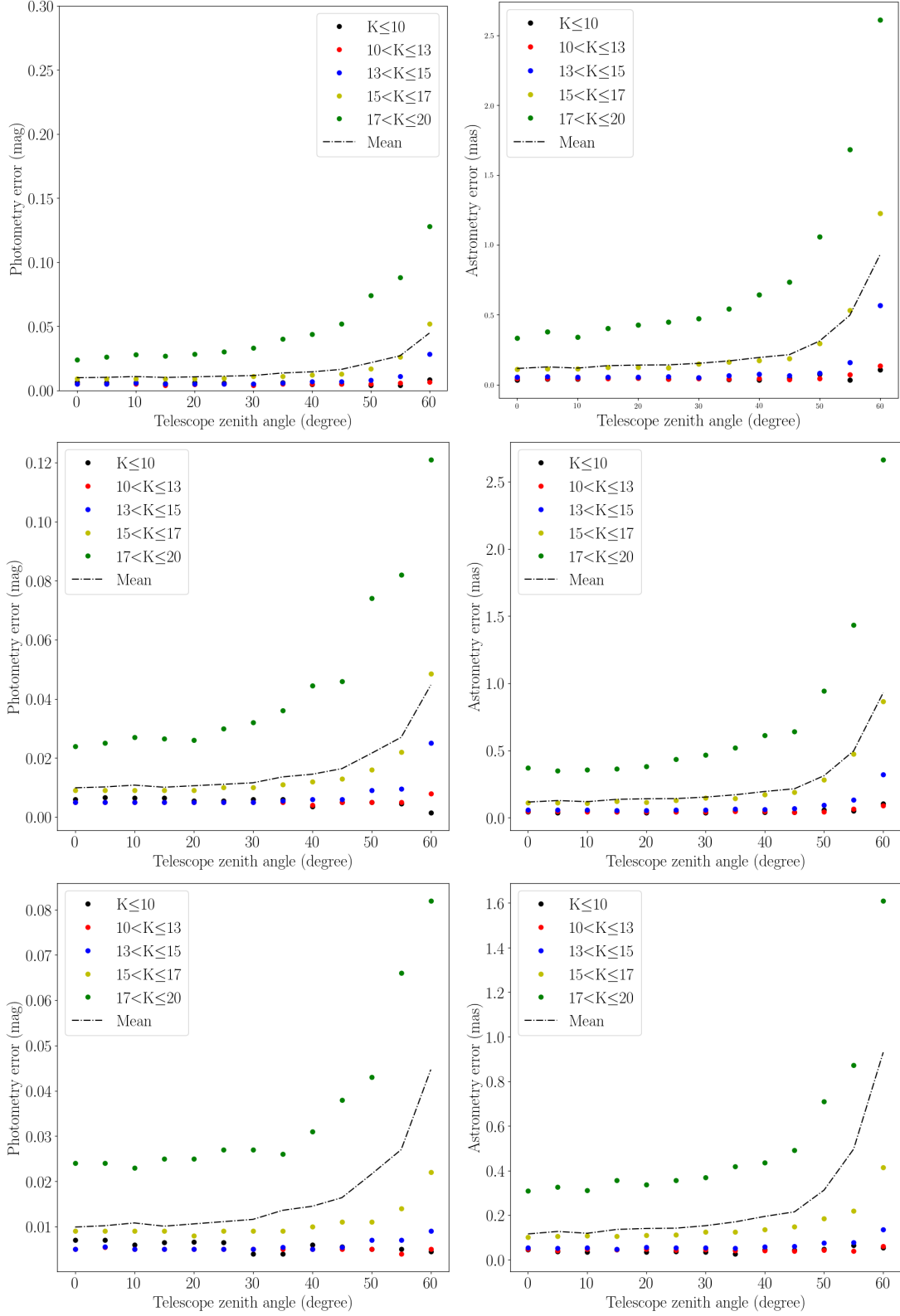


Figure 9: Best-values of photometry and astrometry errors obtained with AIROPA as function of the telescope zenith angle for **Top:**  $r_0 = 8$  cm **Middle:**  $r_0 = 12$  cm **Bottom:**  $r_0 = 16$  cm, without PSF model errors, i.e. the prior PSF grid was identical to the reference grid generated from the 35 layers  $C_n^2(h)$ .

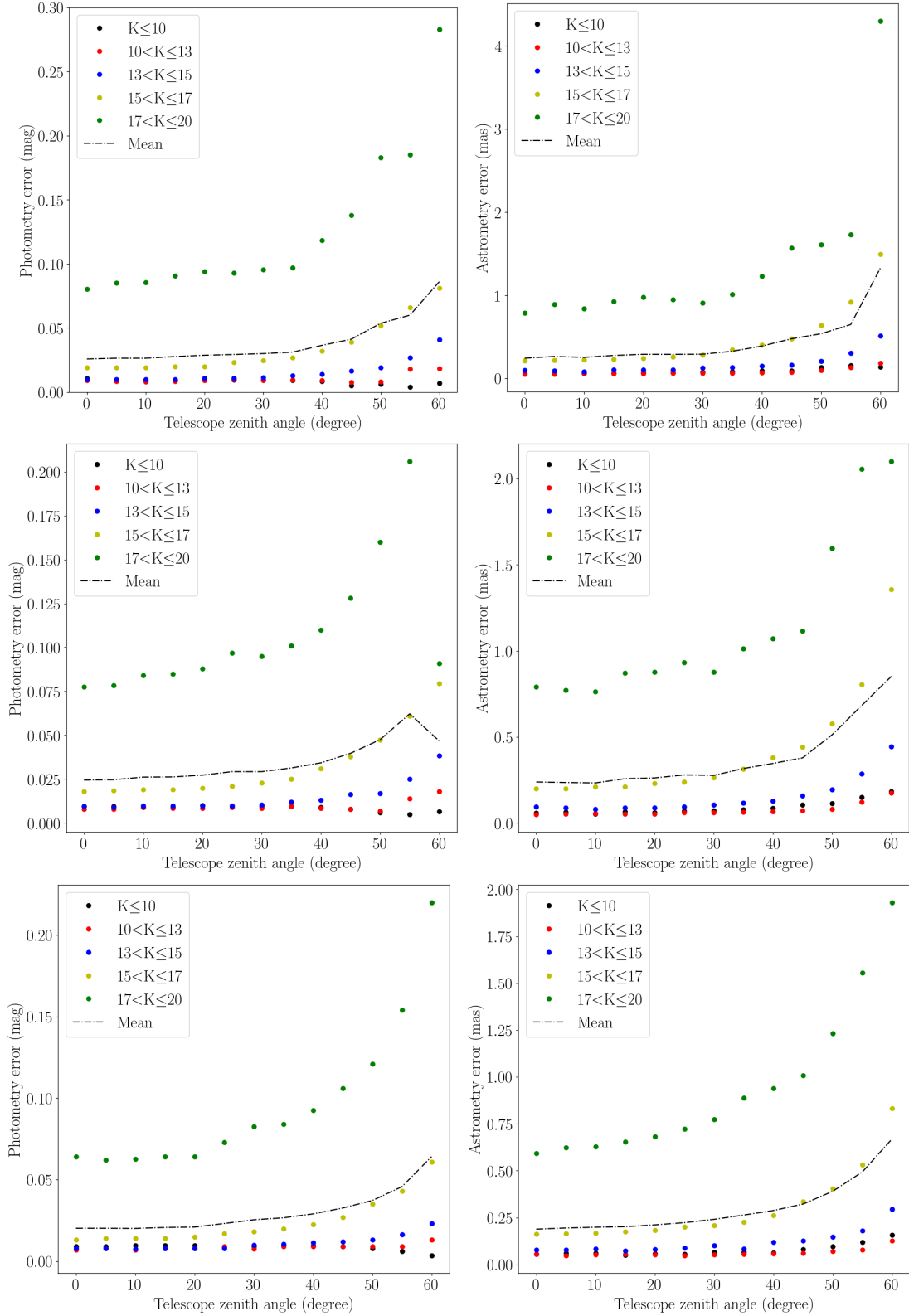


Figure 10: Photometry and astrometry errors obtained with AIROPA as function of the telescope zenith angle for **Top:**  $r_0 = 8$  cm **Middle:**  $r_0 = 12$  cm **Bottom:**  $r_0 = 16$  cm, based on a 7-layers compressed profile with the MASS/DIMM vertical resolution.

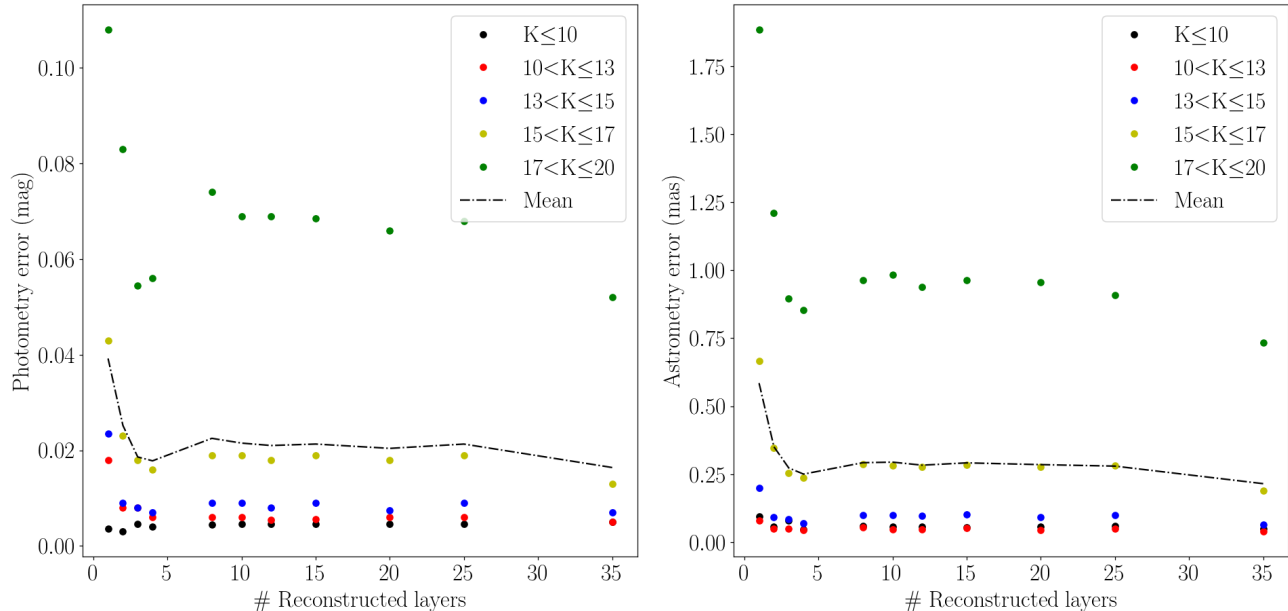


Figure 11: Photometry and astrometry errors obtained with AIROPA for  $r_0 = 8$  cm as function of the number of reconstructed turbulence layers, e.g. the number of layers used to compress the 35-layers profile using a mean-weighted approach that conserves both isoplanatic angle and seeing values.

at their best achievement. Having a correct estimation of  $\theta_0$  is therefore mandatory, which is not necessarily an exclusive conditions, though. Regarding that  $\theta_0 \propto r_0/\bar{h}$ , with  $\bar{h}$  the mean-altitude defined by

$$\bar{h} = \left( \frac{\int_0^\infty h^{5/3} C_n^2(h) dh}{\int_0^\infty C_n^2(h) dh} \right)^{3/5}, \quad (6)$$

we must obtain first a proper estimation of  $r_0$ , which is supposed to be ensured thanks to the DIMM, plus a correction estimation of  $\bar{h}$ . Therefore, if the  $C_n^2(h)$  is correctly estimated at the discrete MASS bin heights, the  $\bar{h}$  will be systematically underestimated by the fact we miss energy at altitudes not sensed by the MASS. On the contrary, if  $\bar{h}$  is rightly assessed, it would mean that the  $C_n^2(h)$  estimated at a particular MASS bin does not comply with the real turbulence strength at this particular bin height. For instance, if the profile contains two layers with  $C_n^2(h = 17 \text{ km}) = 10^{-13} \text{ m}^{1/3}$  and  $C_n^2(h = 15 \text{ km}) = 10^{-14} \text{ m}^{1/3}$ , neither estimate  $C_n^2(h = 16 \text{ km}) = 0$  nor  $0.5 \cdot 10^{-13} \text{ m}^{1/3}$  will produce the same PSF spatial variations. To achieve this, we should rely on a highly resolved profile, as provided by the stereo-SCIDAR for instance (23). However, such an instrument is not systematically available during science observations, suggesting that another path must be also explored alternatively to enhance the anisoplanatism characterization.

A relevant option would be to deploy PRIME that combines PSF-R and PSF extraction to calibrate a PSF model entries, such as the  $C_n^2(h)$  or low-order modes aberrations. We invite the reader to refer to<sup>19</sup> and the poster/proceedings in this conference. By assuming we are capable of extracting some PSFs or sub-field from the on-sky image, two options are feasible

- 1 We have AO control loop data: we can reconstruct the PSF and calibrate some atmosphere/system parameters over the extracted sub-field in order to provide a PSF model at any position in the field and spectrum
- 2 We do not have AO control loop: we can estimate the on-axis OTF using AIROPA and use the Focal Plan Profiling (12) technique to evaluate the  $C_n^2$  profile over few layers, depending on the field and imaging wavelength (6). This would provide an autonomous estimation of the atmospheric vertical profile and ensure that the PSF shape and its spatial variations are ultimately well calibrated.

## 4. CONCLUSION

We have presented a sensitivity analysis of the AIROPA pipeline dedicated to stellar parameters measurements on AO-corrected images. Comparatively to the native pipeline Starfinder, AIROPA does include a model of spatial variations, e.g. anisoplanatism and field-dependent aberrations. As conclusion, we must retain that

- Taking into account PSF spatial variations allows to unbiased stellar parameters estimation and increase their precision by a factor 3 at least.
- Some residual remains, even when PSF spatial variations are perfectly known. We must determine whether this comes from the S/N or from an intrinsic limitation.
- Calibrated field-dependent aberrations show the presence of a strong field curvature: the focus term rms value grows up to 140 nm across 6 arcsec, with a slope of 3.6 nm/arcsec<sup>2</sup>
- Error on the z-position control of the fiber-stage may degrade the PSF model accuracy and therefore the stellar characteristics assessment as well by up to a factor 4. However, as long as the fiber stage is controlled with a 10  $\mu$ m accuracy as expected, this degradation should not exceed more than 6 %.
- Anisoplanatism does not play a major role regarding both imaging wavelength and field size, except for high telescope elevation accumulated with bad seeing conditions. Describing the  $C_n^2$  profile over three layers is enough, as long as we rely on an approach that conserves the isoplanatism angle, e.g. either a high vertical resolution measurement at fixed altitude or an estimation that retrieves bin height and strength.

Future work will be dedicated to improve AIROPA and push further science verification.

## ACKNOWLEDGMENTS

The research leading to these results received the support of the A\*MIDEX project (no. ANR-11-IDEX-0001-02) funded by the Investissements d’Avenir French Government program, managed by the French National Research Agency (ANR). This work has received partial funding from the European Unions Horizon 2020 research and innovation programme under grant agreement No 730890. This work was also supported by the Action Spécifique Haute Résolution Angulaire (ASHRA) of CNRS/INSU co-funded by CNES.

## REFERENCES

- [1] Schödel, R., “Accurate photometry with adaptive optics in the presence of anisoplanatic effects with a sparsely sampled PSF. The Galactic center as an example of a challenging target for accurate AO photometry,” *Astron. & Astrophys.* **509**, A58 (Jan. 2010).
- [2] Yelda, S., Lu, J. R., Ghez, A. M., Clarkson, W., Anderson, J., Do, T., and Matthews, K., “Improving Galactic Center Astrometry by Reducing the Effects of Geometric Distortion,” *The Astrophysical Journal* **725**, 331–352 (Dec. 2010).
- [3] Ragland, S., Dupuy, T. J., Jolissaint, L., Wizinowich, P. L., Lu, J. R., van Dam, M. A., Berriman, G. B., Best, W., Gelino, C. R., Ghez, A. M., Liu, M. C., Mader, J. A., Vayner, A., Witzel, G., and Wright, S. A., “Status of point spread function determination for Keck adaptive optics,” in [*Adaptive Optics Systems VI*], *Proc. SPIE* **10703**, 107031J (July 2018).
- [4] Jolissaint, L., Ragland, S., and Wizinowich, P., “Adaptive Optics Point Spread Function Reconstruction at W. M. Keck Observatory in Laser Natural Guide Star Modes : Final Developments,” in [*Adaptive Optics for Extremely Large Telescopes IV (AO4ELT4)*], E93 (Oct. 2015).
- [5] Sitarski, B. N., Witzel, G., Fitzgerald, M., Meyer, L., Ghez, A. M., Campbell, R. D., Lu, J. R., M. K., Wizinowich, P., and Lyke, J., “Modeling instrumental field-dependent aberrations in the nirc2 instrument on the keck ii telescope,” in [*Adaptive Optics Systems IV*], *Proc. SPIE* **9148** (August 2014).
- [6] Beltramo-Martin, O., Correia, C. M., Mieda, E., Neichel, B., Fusco, T., Witzel, G., Lu, J. R., and Véran, J.-P., “Off-axis point spread function characterization in laser guide star adaptive optics systems,” *M.N.R.A.S* **478**, 4642–4656 (Aug. 2018).

- [7] Britton, M. C., “The Anisoplanatic Point-Spread Function in Adaptive Optics,” *Publications of the Astronomical Society of the Pacific* **118**, 885–900 (June 2006).
- [8] Ciurlo, A., Do, T., Witzel, G., Lu, J., Lyke, J., Fitzgerald, M. P., Ghez, A., Campbell, R., and Turri, P., “Off-axis PSF reconstruction for integral field spectrograph: instrumental aberrations and application to Keck/OSIRIS data,” in [*Adaptive optics systems VI*], *Proc. SPIE* **10703**, 107031O (July 2018).
- [9] Witzel, G., Lu, J. R., Ghez, A. M., Martinez, G. D., Fitzgerald, M. P., Britton, M., Sitarski, B. N., Do, T., Campbell, R. D., Service, M., Matthews, K., Morris, M. R., Becklin, E. E., Wizinowich, P. L., Ragland, S., Doppmann, G., Neyman, C., Lyke, J., Kassis, M., Rizzi, L., Lilley, S., and Rampy, R., “The AIROPA software package: milestones for testing general relativity in the strong gravity regime with AO,” in [*Adaptive Optics Systems V*], *Proc. SPIE* **9909**, 99091O (July 2016).
- [10] Diolaiti, E., Bendinelli, O., Bonaccini, D., Close, L. M., Currie, D. G., and Parmeggiani, G., “StarFinder: A code for stellar field analysis.” Astrophysics Source Code Library (Nov. 2000).
- [11] Butterley, T., Sarazin, M., Navarrete, J., Osborn, J., Farley, O., and Le Louarn, M., “Improvements to MASS turbulence profile estimation at Paranal,” in [*Proc. SPIE* ], *Society of Photo-Optical Instrumentation Engineers (SPIE) Conference Series* **10703**, 107036G (Jul 2018).
- [12] Beltramo-Martin, O., Correia, C. M., Neichel, B., and Fusco, T., “Focal-plane  $C_n^2(h)$  profiling based on single-conjugate adaptive optics compensated images,” *M.N.R.A.S* **481**, 2349–2360 (Dec. 2018).
- [13] Veran, J.-P., Rigaut, F., Maitre, H., and Rouan, D., “Estimation of the adaptive optics long-exposure point-spread function using control loop data.,” *Journal of the Optical Society of America A* **14**, 3057–3069 (Nov. 1997).
- [14] Gendron, E., Clénet, Y., Fusco, T., and Rousset, G., “New algorithms for adaptive optics point-spread function reconstruction,” *Astron. & Astrophys.* **457**, 359–363 (Oct. 2006).
- [15] Flicker, R., “PSF reconstruction for Keck AO,” tech. rep., W.M. Keck Observatory, 65-1120 Mamalahoa Hwy, Waimea, HI 96743, United-States (2008).
- [16] Gilles, L., Correia, C., Véran, J.-P., Wang, L., and Ellerbroek, B., “Simulation model based approach for long exposure atmospheric point spread function reconstruction for laser guide star multiconjugate adaptive optics,” *Appl. Opt.* **51**, 7443–7458 (Nov 2012).
- [17] Martin, O. A., Correia, C. M., Gendron, E., Rousset, G., Gratadour, D., Vidal, F., Morris, T. J., Basden, A. G., Myers, R. M., Neichel, B., and Fusco, T., “Point spread function reconstruction validated using on-sky CANARY data in multiobject adaptive optics mode,” *Journal of Astronomical Telescopes, Instruments, and Systems* **2**, 048001 (Oct. 2016).
- [18] Fétick, R. J., Fusco, T., Neichel, B., Mugnier, L., Beltramo-Martin, O., Bonnefois, A., Petit, C., Milli, J., Vernet, J., S., O., and Bacon, R., “Physics-based model of the adaptive-optics-corrected point spread function,” * * (2019).
- [19] Beltramo-Martin, O., Correia, C. M., Ragland, S., Jolissaint, L., Neichel, B., Fusco, T., and Wizinowich, P., “PRIME: Psf Reconstruction and Identification for Multiple sources characterization Enhancement. Application to Keck NIRC2 imager,” *M.N.R.A.S* (2019).
- [20] Fried, D. L., “Anisoplanatism in adaptive optics,” *Journal of the Optical Society of America (1917-1983)* **72**, 52 (Jan. 1982).
- [21] Sarazin, M., Le Louarn, M., Ascenso, J., Lombardi, G., and Navarrete, J., “Defining reference turbulence profiles for E-ELT AO performance simulations,” in [*Proceedings of the Third AO4ELT Conference*], Esposito, S. and Fini, L., eds., 89 (Dec. 2013).
- [22] Costille, A. and Fusco, T., [*Impact of  $C_n^2$  profile on tomographic reconstruction performance: application to E-ELT wide field AO systems*], vol. 8447 of *Proc. SPIE* (July 2012).
- [23] Osborn, J., Wilson, R. W., Sarazin, M., Butterley, T., Chacón, A., Derie, F., Farley, O. J. D., Haubois, X., Laidlaw, D., LeLouarn, M., Masciadri, E., Milli, J., Navarrete, J., and Townson, M. J., “Optical turbulence profiling with Stereo-SCIDAR for VLT and ELT,” *M.N.R.A.S* **478**, 825–834 (July 2018).